Geotech Geol Eng (2014) 32:1187–1210
DOI 10.1007/s10706-014-9789-9

ORIGINAL PAPER

Trial Embankment Analysis to Predict Smear Zone Characteristics Induced by Prefabricated Vertical Drain Installation

Ali Parsa-Pajouh · Behzad Fatahi · Philippe Vincent · Hadi Khabbaz

Received: 11 February 2014 / Accepted: 31 May 2014 / Published online: 15 June 2014

Abstract In this study, FLAC finite difference software has been adopted to simulate the performance of the ground improved using prefabricated vertical drains assisted preloading, considering smear zone characteristics. The numerical code has been applied to predict smear zone properties employing a back calculation procedure using the results of several case studies. The construction of a trial embankment is proposed as a reliable method to predict the smear zone characteristics. The proposed back calculation method is applied to estimate the minimum required degree of consolidation and consequently the minimum required preloading time, resulting in a reliable estimation of the smear zone permeability and extent. Three preloading case studies considering both conventional preloading and vacuum assisted preloading have been simulated to verify the numerical code and to conduct the parametric study using the back calculation procedure. According to the results, the properties of the smear zone can be back-calculated reliably, when at least 33 % degree of consolidation due to trial embankment construction is achieved.

Keywords Vertical drain · Smear zone · Trial embankment · Numerical modeling · FLAC · Soft soil · Ballina clay

1 Introduction

Preloading with prefabricated vertical drains (PVDs) is highly recommended as an effective ground improvement technique in deep soft soil deposits (e.g. Abuel-Naga et al. 2006; Rowe and Taechakumthorn 2008). Installation of vertical drains reduces the drainage path to half length of the effective drain spacing, accelerating the consolidation settlement rate significantly as the consolidation time is inversely proportional to the square of the drainage path. Preloading can be combined with the vacuum pressure to accelerate the settlement rate and rectify the embankment stability problems because of reduced embankment height. Vacuum preloading using membrane is a common ground improvement technique, which consists of vertical drains and a drainage sand blanket on top sealed from atmosphere by an impervious membrane on the top. Horizontal drains are installed in the drainage layer and connected to a vacuum pump. Negative pressures are created in the drainage layer by means of the vacuum pump. The applied negative pressure generates negative pore water pressures, resulting in an increase in the effective stress in the soil, which in turn leads to an

A. Parsa-Pajouh · B. Fatahi (✉) · H. Khabbaz
School of Civil and Environmental Engineering, University of Technology Sydney (UTS), City Campus, Broadway, Sydney, NSW 2007, Australia
e-mail: behzad.fatahi@uts.edu.au

P. Vincent
Menard Bachy Pty Ltd, Sydney, Australia

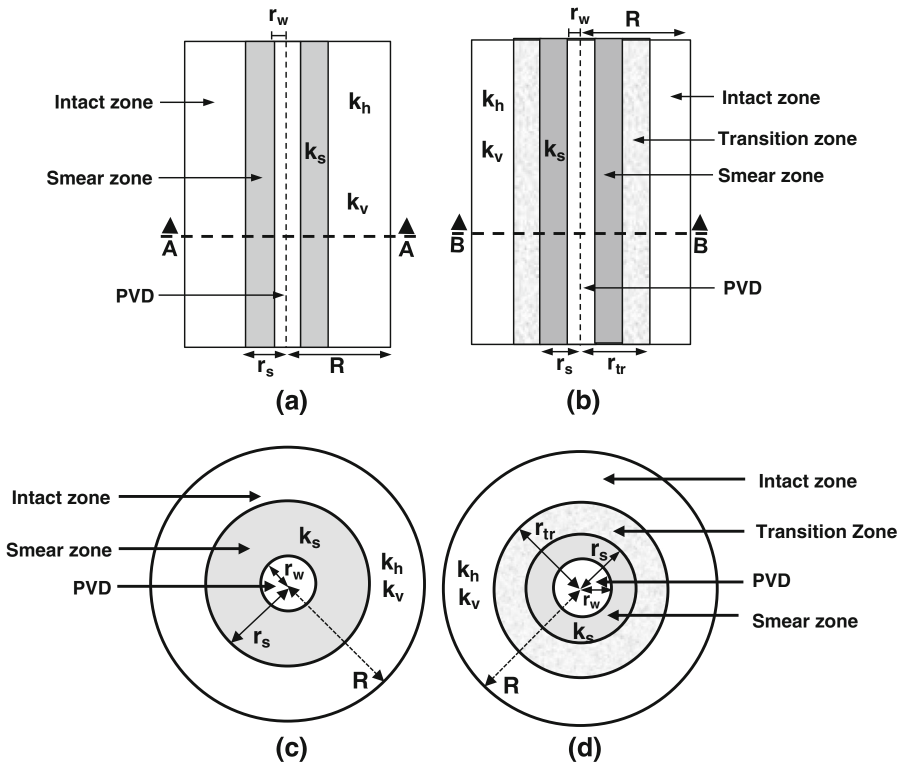

Fig. 1 PVD surrounding by smear zone, (**a**) profile, two zones hypothesis; (**b**) profile, three zones hypothesis; (**c**) cross-section A–A, two zones hypothesis; (**d**) cross-section B–B, three zones hypothesis

accelerated consolidation process. This method has been successfully used for soil improvement or land reclamation projects in different countries (Saowapakpiboon et al. 2009; Kelly and Wong 2009; Indraratna et al. 2011).

Prefabricated vertical drains (PVDs) are installed using mandrel. Mandrel insertion disturbs the soil around the drain to a certain extent and reduces the soil permeability in this region, which is called smear zone. The presence of the smear zone significantly influences the horizontal consolidation rate (Sharma and Xiao 2000; Basu and Prezzi 2007). According to literature, two main hypotheses are proposed to characterise the disturbed soil surrounding the drain; (a) two zones hypothesis (Chai and Miura 1999; Indraratna and Redana 1997; Rujikiatkamjorn and Indraratna 2009), which divides the surrounding soil into the smear zone, and the intact zone and (b) three zones hypothesis (Hawlader and Muhunthan 2002; Basu et al. 2006), considering three zones, which are the smear zone in the immediate vicinity of the drain, the transition zone, and the undisturbed zone. Figure 1 illustrates the profile and the cross section of the ground in the vicinity of the vertical drain for both hypotheses.

In the two zone hypothesis, two major parameters are proposed to characterise the smear zone; the extent ratio (s) and the permeability ratio (n):

$$s = r_s/r_m \quad or \quad r_s/r_w \tag{1}$$

$$n = k_h/k_s \tag{2}$$

where, r_s is the radius of the smear zone, r_m is the radius of the mandrel, r_w is the radius of the vertical drain, k_h is the horizontal permeability of the intact zone, and k_s is the permeability of the smear zone. It should be noted that usually it is assumed that vertical and horizontal permeability values in the smear zone are the same (Indraratna and Redana 1998).

Determination of r_s/r_m and k_h/k_s is a challenging task because of many uncertainties involved (Chai and Miura 1999; Hansbo 1997). Observed results from pilot tests or past projects in similar ground conditions are often used to estimate these parameters, which are not always consistent (Hansbo 1997). It is also difficult to distinguish the influence of the smear zone from other influencing factors such as well resistance and transmissivity of the drainage mat (Sharma and Xiao 2000). Therefore, a number of large-scale instrumented

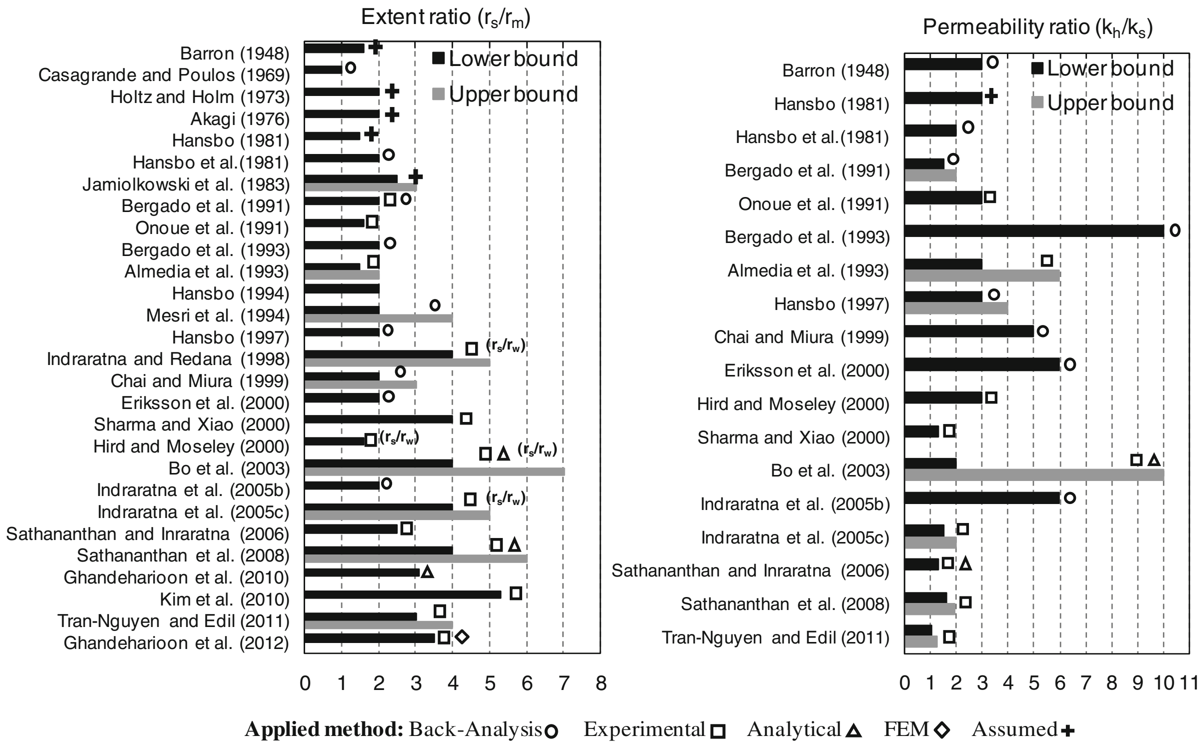

Fig. 2 Proposed values for smear zone characteristics

laboratory tests have been conducted to characterise the smearing effect and determine the smear zone permeability and extent (Indraratna and Redana 1998; Saowapakpiboon et al. 2011; Sharma and Xiao 2000; Tran-Nguyen and Edil 2011). According to literature, very diverse values are reported for the permeability ratio (n) and extent ratio (s), which are illustrated in Fig. 2. The proposed range shows that the extent of the smear zone (r_s) may vary from 1.6 to 7 times of the drain radius (r_w) or 1 to 6 times of the mandrel equivalent diameter (r_m). The proposed range for the permeability ratio (k_h/k_s) is 1.3–10.

It can be observed that wide ranges are proposed for k_h/k_s and r_s/r_m and there is no comprehensive method to predict these parameters precisely to be used by practising engineers. The assumptive properties for smear zone characteristics may result in inaccurate predictions of the ground behaviour. This can lead to the early removal of the surcharge in the construction process resulting in excessive post construction settlement or excessive construction time increasing the project cost.

Simulation of the PVD assisted preloading process for the complex ground conditions at laboratory to estimate the smear zone characteristics is a challenging task as many uncertainties are involved and final results may not be reliable for the practical design purposes. Furthermore, most of the analytical solutions are developed based on the assumption of a single axisymmetric drainage system and cannot be applied to analyse the behaviour of the soft soil deposit improved with multiple vertical drains (Indraratna and Redana 2000). These limitations can be magnified when the subsurface soil has the multi-layer profile. Field monitoring of the actual preloading projects in combination with the numerical analysis offers an opportunity to investigate the consolidation behaviour of the soft soil and back calculate the smear zone properties precisely. Construction of a fully instrumented trial embankment has been used extensively as a reliable method to determine the feasibility of preloading with vertical drains and to estimate the smear zone properties applying a back calculation procedure (Kelly 2008). A selected number of constructed trial embankments combined with vertical drains and vacuum pressure are summarised in Table 1.

The long trial embankment construction time is the major challenge in using this method to conduct the

Table 1 Case histories—trial embankments stabilised by prefabricated vertical drains

Title	Location	Type	PVD installation pattern	Drain spacing (m)	Soft soil depth (m)	Reference
Porto Tolle	Italy	PVD	Triangular	3.8	21.5	Hird et al. (1995)
Second Bangkok international Airport	Thailand	PVD	Triangular	1.0	16.0	Bergado et al. (1998)
Muar site	Malaysia	PVD	Triangular Square	1.3–2.0	20.0	Balasubramaniam et al. (2007)
Tianjin Port	China	PVD + Vacuum	Square	1.0	20.0	Yan and Chu (2005)
Gangavaram Port	India	PVD	Triangular	1.0–1.5	10.0–18.0	Bhosle and Vaishampayan (2009)
Veda	Sweden	PVD	Triangular	1.07	10.0	Muller and Larssen (2009)
Survarnabhumi Airport	Thailand	PVD + vacuum	Triangular	0.85	10.0	Saowapakpiboon et al. (2009)
Port of Brisbane	Australia	PVD + Vacuum	Square	1.2	18.0	Indraratna et al. (2011)

back calculation analysis and estimate the smear zone permeability and extent, and in many cases may cause a considerable delay in the construction of the actual embankment and a significant increase in the project cost. Estimation of the smear zone permeability and extent in the early stages of the trial embankment construction can convert this method to a very practical, accurate and cost effective approach. In this study, a back analysis procedure is proposed to determine the properties of the smear zone. Furthermore, the minimum degree of consolidation (minimum preloading time), resulting in well-predicted smear zone properties is estimated. A numerical procedure adopting FLAC 2D software has been applied to simulate the PVD assisted preloading case studies and back analyse the smear zone characteristics for the design.

2 Numerical Modelling and Back Calculation Procedure

Numerical analysis methods have been widely employed by geotechnical engineers to rectify the limitations of the analytical approaches in simulation of the complex PVD assisted preloading projects to predict the ground behaviour, conduct the parametric studies and back calculate the smear zone properties. Literature shows that CRISP, ABAQUS, and PLAXIS are the most commonly used programs, by researchers to conduct the numerical simulation (Chai and Miura 1999; Indraratna et al. 2005a; Saowapakpiboon et al. 2011; Sathananthan et al. 2008; Stapelfeldt et al. 2008; Fatahi et al. 2009 and 2010; Fatahi et al. 2012a). In this study FLAC software has been employed to conduct the numerical analysis. FLAC 2D is a two-dimensional explicit finite difference program for engineering mechanics computation, which uses the mixed discretisation scheme developed by Marti and Cundall (1982) for accurate modeling of plastic deformations and flow. In addition, the employed explicit solution scheme used in FLAC in contrast to the common implicit methods can compute any material nonlinearity behaviour in almost the same computation time as a linear law (Tabatabaiefar et al. 2013a, b; Hokmabadi et al. 2014a, b). In this study, FLAC 2D (Ver. 6) has been adopted to develop the numerical code and simulate the performance of the ground improved using PVD assisted preloading taking the advantages of FLAC's built-in programming language FISH. The developed finite difference model includes: (1) two-dimensional plane-strain model, (2) the explicit, Lagrangian calculation scheme and the mixed-discretization zoning technique ensuring the accuracy of the plastic collapse and flow modeling, (3) Biot theory of consolidation for the formulation of coupled fluid-deformation mechanisms (Biot 1941), and (4) modified Cam-Clay (MCC) constitutive model to simulate the behaviour of the soft soil (Roscoe and Burland 1968). Required new subroutines have been

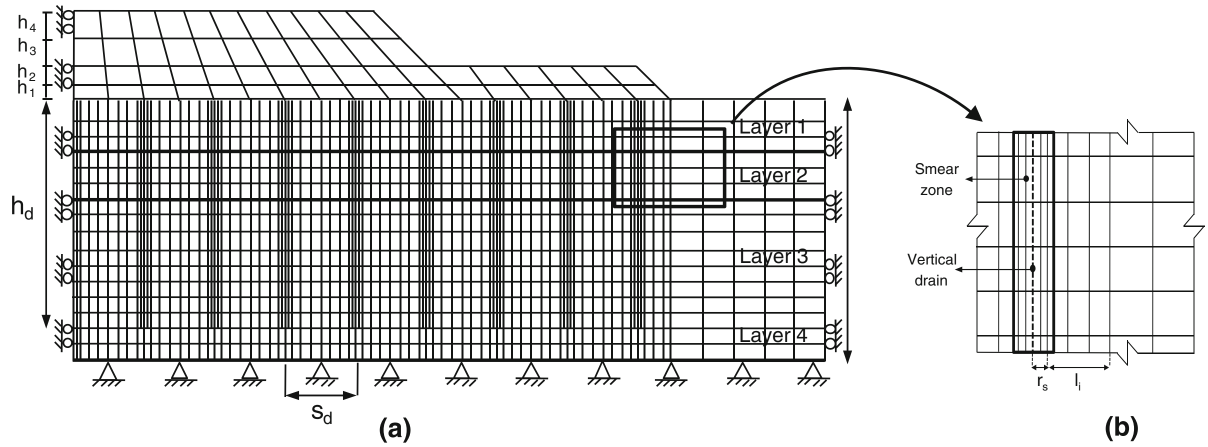

Fig. 3 **a** A sample of generated finite-element mesh employing the developed code; **b** the pattern of meshes in the smear zone and undisturbed region (r_s = smear zone extent; I_i = intact zone extent; h_t = height of soil profile; and h_d = length of the vertical drain)

written using the built-in programming language FISH (FLACish) to tailor analyses to suit specific needs for the parametric study. Figure 3 shows a sample of generated meshes for an embankment applying the developed code.

Construction of a trial embankment can be applied as a practical and reliable solution to analyse the smearing effects on the preloading process and predict the smear zone properties using a back calculation approach. In this study, a systematic back calculation procedure is designed to define the smear zone properties (Fig. 4) employing the field measurements. In addition, the developed back calculation procedure is employed to define the minimum required degree of consolidation for trial embankment construction to be used to obtain the smear zone properties.

Figure 4 presents detailed flowchart, including the back calculation procedure to find the smear zone characteristics and the minimum time, required to monitor the trial embankment. The proposed back calculation procedure has three stages, (1) entering the input data, including the ground conditions, soil properties, PVD installation details, and the upper and lower bound values for the smear zone properties (r_s/r_m and k_h/k_s); (2) conducting the numerical analysis varying r_s/r_m and k_h/k_s in the given range to predict the ground behaviour, determining the corresponding settlement curves, and calculating the accumulative error between numerical results and field measurements at every degree of consolidation; (3) analysing the outcomes of the second stage to define the optimum combination of r_s/r_m and k_h/k_s resulting in the best predicted settlement curve, which is in the best agreement with the field measurements and determining the minimum required waiting time after construction of trial embankment to find those parameters. Thus, the minimum total accumulative prediction errors should be plotted against the degree of consolidation. The minimum required degree of consolidation and corresponding time belong to the point with the minimum accumulative prediction error, which can be reported as the minimum required preloading time. The predicted smear zone properties (r_s/r_m and k_h/k_s) at that point can be reported as the reliable parameters for the practical design purposes.

Three case studies of PVD assisted preloading projects in Australia including: (1) the 8.5 m height Ballina Bypass trial embankment, (2) the 5.0 m height Cumbalum trial embankment, and (3) the 2.85 m Sunshine trial embankment, are selected for the numerical simulations, verification of the developed code, and conducting the parametric studies adopting the back analysis procedure.

3 Case Studies

3.1 Case Study 1: Ballina Bypass Vacuum Trial Embankment

The Ballina Bypass is a part of the Pacific Highway upgrade at New South Wales, Australia and traverses a flood plain associated with the Richmond River and its tributary creeks. Soft soil deposits within the flood

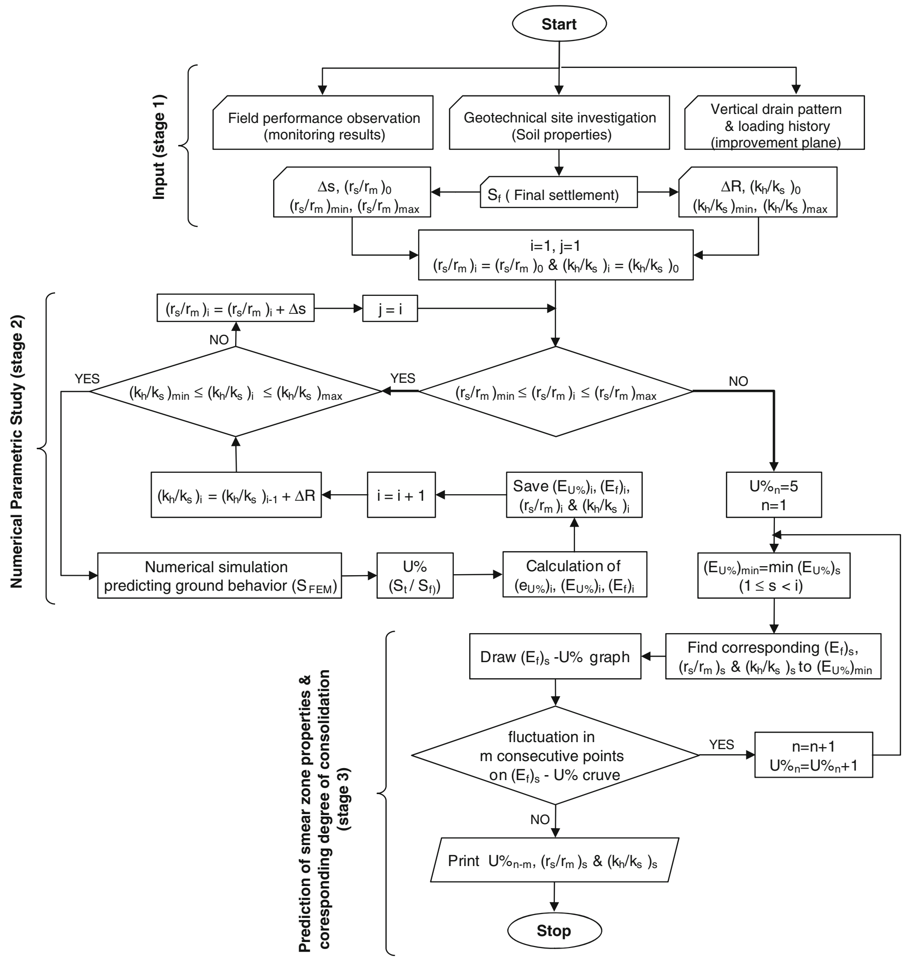

$(r_s/r_m)_0$	assumed initial extent ratio	ΔR	permeability ratio increment depending on the required accuracy
$(k_h/k_s)_0$	assumed initial permeability ratio	ΔS	extent ratio increment depending on the required accuracy
$(r_s/r_m)_{min}$	minimum extent ratio	U%	degree of consolidation at time t ($U\%=S_t / S_f$)
$(r_s/r_m)_{max}$	maximum extent ratio	$(e_{U\%})_i$	error between numerical predictions and field results at U% at step i
$(k_h/k_s)_{min}$	minimum permeability ratio	$(E_{U\%})_i$	accumulative error at U% at step i
$(k_h/k_s)_{max}$	maximum permeability ratio	$(E_f)_i$	final accumulative error at step i
$(r_s/r_m)_i$	extent ratio at step i	$(E_{U\%})_{min}$	minimum accumulative error at U% corresponding to step s (1<s<i)
$(k_h/k_s)_i$	permeability ratio at step i	$(E_f)_s$	final accumulative error corresponding to step s having $(E_{U\%})_{min}$
S_t	field measurements at time t	$(r_s/r_m)_s$	extent ratio corresponding to step s that gives the minimum error
S_{FDM}	numerical predictions	$(k_h/k_s)_s$	permeability ratio corresponding to step s that gives $(E_{U\%})_{min}$
S_f	final settlement	$U\%_{n-m}$	degree of consolidation corresponding to step n-m
i& n	counters	m	number of successive points on $(E_f)_s$ –U% curve with no fluctuations

Fig. 4 Back calculation flowchart for smear zone characteristics and the minimum required monitoring time for trial embankment

plain can be up to 25 m thick. Vacuum consolidation was identified as a ground improvement technique that permitted more rapid construction than surcharge and PVDs as well as being potentially more cost effective than ground inclusions (Kelly and Wong 2009). A trial embankment at north-west of Ballina was constructed to investigate the performance of this approach. Construction of the trial embankment started with placement of 1.5 m sand layer with the unit weight of 21.5 kN/m^3 to act as a working platform for plants as well as the drainage layer. Then 34 mm diameter circular vertical drains were installed with the spacing of 1.0 m in square

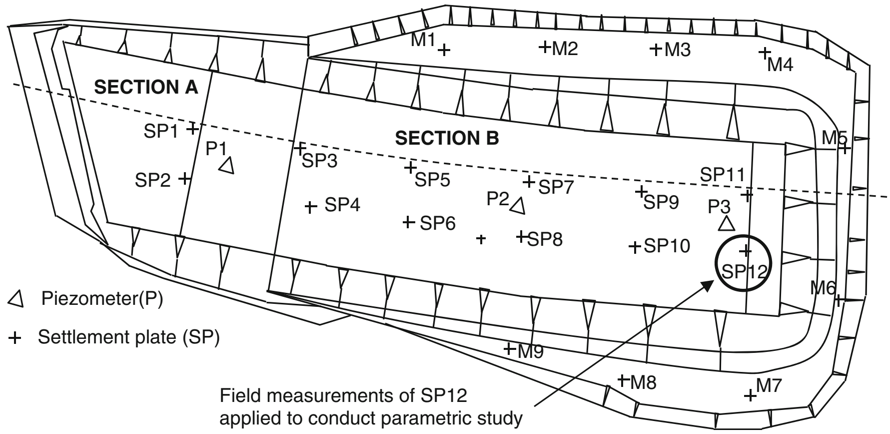

Fig. 5 Instrumentation layout for the trial embankment at Ballina Bypass

pattern, which were connected to the horizontal drains. After instrumentation, a layer of fine grained sand placed on top of the granular material to protect the membrane. Then the membrane was installed having a layer of fine grain sand on top to be protected from punctures, and general fill was then placed on top of the sand layer. The embankment was separated into two sections, namely Section A, the non-vacuum area and Section B, the vacuum area. Figure 5 illustrates the location of the field instrumentation, including surface settlement plates and piezometers. Field measurements at settlement plate No. 12 (SP12) and piezometer P3 in Section B in conjunction with the soil profile data have been used to verify the developed FLAC code.

The embankment was constructed in stages using a granular material ($\gamma_s = 20$ kN/m^3) up to a height of 8.5 m. A detailed cross section of the embankment and subsoil profile (at the location of SP12) is shown in Fig. 6. A vacuum pressure of 70 kPa was applied for a period of 400 days and then removed. The construction history of the trial embankment is demonstrated in Fig. 7. The soft soil deposit was in a lightly over consolidated state with an over-consolidation ratio (OCR) of 2.5 for the surface crust (0.5 m tick) and less than 2 for the rest of the layers. The adopted parameters for the subsoil layers based on the site investigation results and laboratory tests employed in the numerical analysis are summarised in Table 2.

The consolidation behaviour of soft clay beneath the Ballina Bypass trial embankment was analysed using the developed FLAC code, incorporating the MCC model. Fully saturated coupled flow-deformation simulation carried out to model the dissipation of pore water pressures. The discretised plane-strain finite difference mesh, composed of quadrilateral elements, is shown in Fig. 8a, where only half of the trial embankment is considered by exploiting the symmetry. FLAC subdivides each quadrilateral element into triangular elements (as shown in Fig. 8b). Pore pressures are assumed to vary linearly in a triangular element. The hydrostatic pore water pressure was considered along the vertical drains (before applying the vacuum pressure) to model the PVD (Fig. 8c). The zero excess pore pressure assumed at the ground surface to model the drainage boundary. According to the field measurements uniform distribution of vacuum pressure has been considered and constant negative pore pressure of −70 kPa was applied along the vertical drain, which is illustrated in Fig. 8b.

As the trial embankment is analysed in the plane-strain condition, it is more appropriate to use the equivalent plane-strain permeability (k_{hp}) in the numerical analysis. For this aim, the proposed equivalent plane-strain conversion formulations by Indraratna and Redana (2000) have been used.

$$(k_{hp}/k_h) = \frac{0.67}{[\ln(n) - 0.75]} \tag{3}$$

$$(k_{sp}/k_{hp}) = \frac{\beta}{(k_{hp}/k_h)[\ln(n/s) + (k_h/k_s)\ln(s) - 0.75] - \alpha} \tag{4}$$

$$\alpha = \frac{2(n-s)^3}{3(n-1)n^2} \tag{5}$$

$$\beta = \frac{2(s-1)}{(n-1)n^2}\left[n(n-s-1) + \frac{1}{3}(s^2+s+1)\right] \tag{6}$$

where, k_h and k_{hp} are axisymmetric and plane-strain horizontal permeability values of the intact zone

Fig. 6 Cross section of the Ballina Bypass trial embankment and subsoil profile

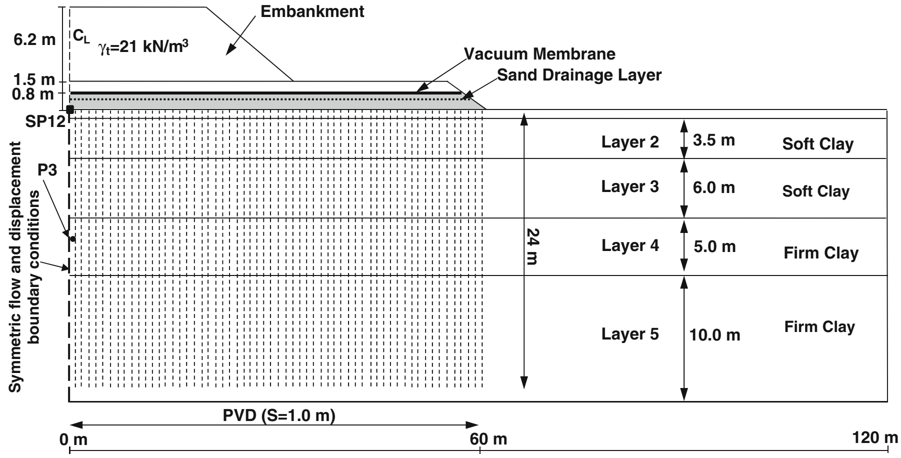

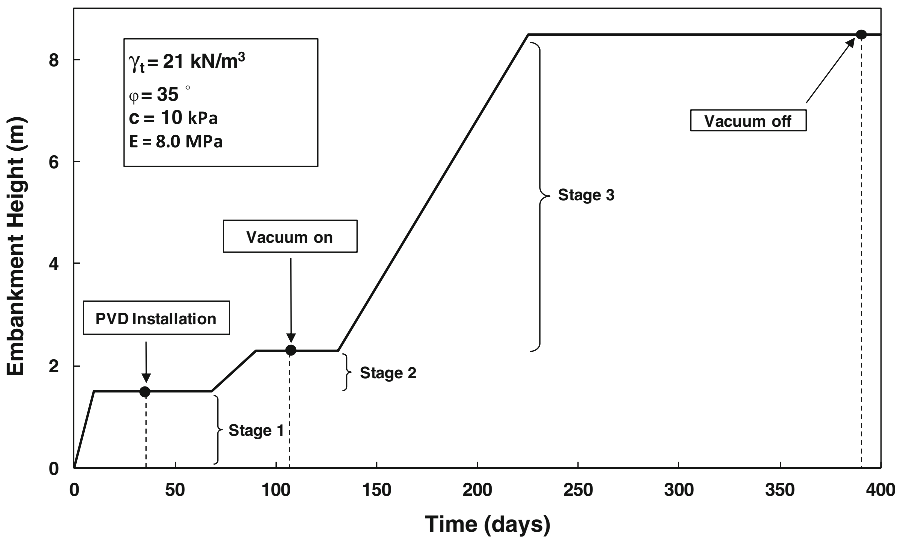

Fig. 7 Construction history of Ballina Bypass trial embankment

Table 2 Adopted properties for subsoil layers for Ballina Bypass trial embankment near SP12

Depth: m	λ	κ	e_0	γ_s (kN/m³)	k_h (10^{-10} m/s)	k_v (10^{-10} m/s)	OCR
0.0–0.5	0.57	0.057	2.75	14.5	3.0	1.5	2.5
0.5–4.0	0.57	0.057	2.75	14.5	6.0	3.0	1.8
4.0–10.0	0.67	0.067	2.87	14.5	6.0	3.0	1.7
10.0–15.0	0.47	0.047	2.61	15.0	15	7.5	1.3
15.0–25.0	0.40	0.040	2.09	15.0	15	7.5	1.2

λ and κ are slopes of the specific volume versus $ln(p')$ curves for compression and swelling, respectively, where p' is the mean effective stress; e_0 is the initial void ratio; γ_s is the unit weight; k_h is the horizontal permeability of intact zone; k_v is the vertical permeability of intact zone; and OCR is the over consolidated ratio

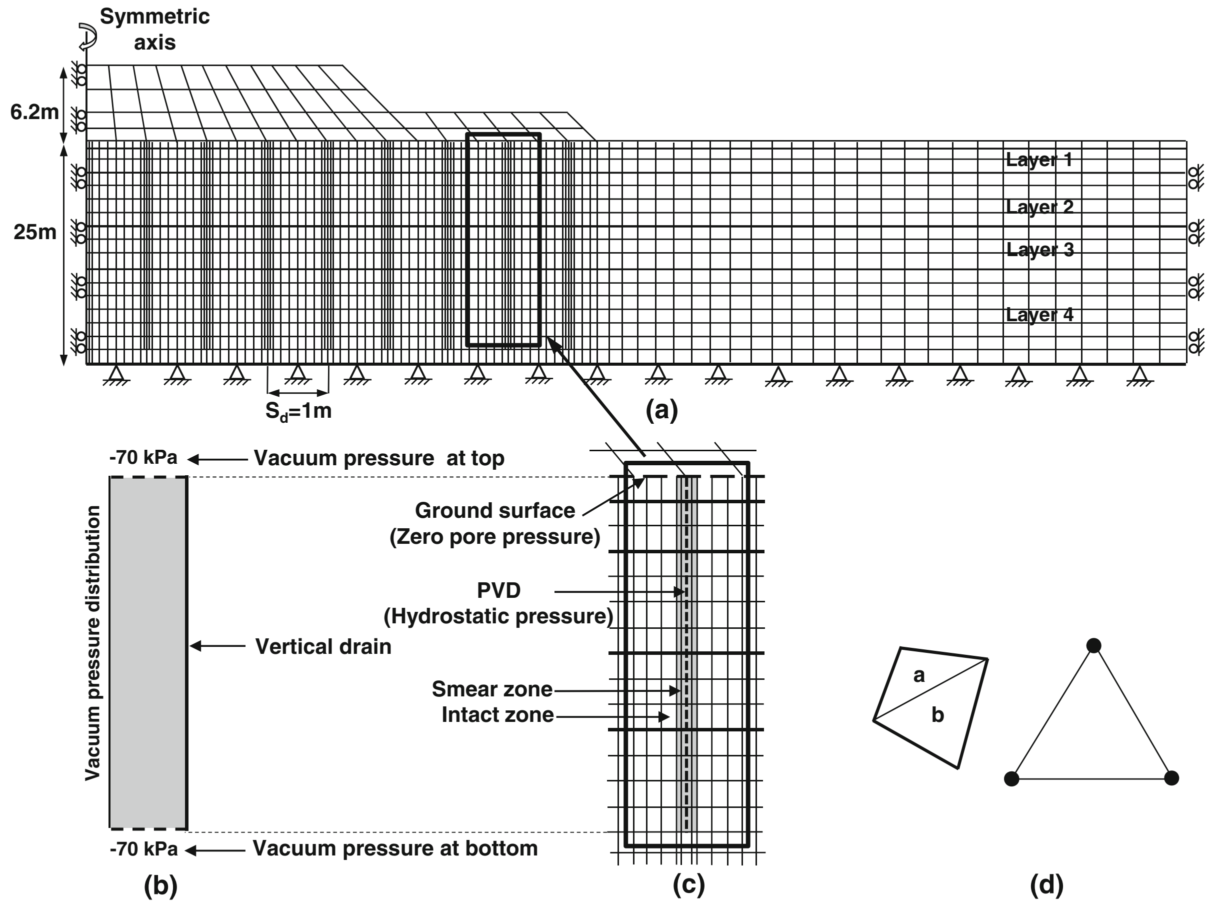

Fig. 8 **a** Discretized finite-difference mesh of Ballina Bypass trial embankment; **b** variation of vacuum pressure along the vertical drain; **c** the pattern of meshes in the smear zone and undisturbed region; **d** FLAC zone composed of overlaid triangular elements

respectively, k_s and k_{sp} are axisymmetric and plane-strain permeability values of the smear zone, respectively, α and β are geometric coefficients, n is the spacing ratio equal to B/b_w, and $s = r_s/r_w$. The value of k_h needs to be determined first (laboratory or field), then k_{hp} can be calculated using Eq. (3). When k_{hp} is known, k_{sp} can be obtained from Eq. (4). Figure 9 shows the axisymmetric and plane-strain profiles of the PVD and the surrounding ground.

The field measurements have been used to verify the FLAC code, which is developed to simulate the PVD assisted preloading with and without the vacuum pressure, considering the smear zone characteristics. In addition, the developed FLAC code has been applied adopting the second stage of the back calculation procedure in Fig. 4, to conduct the parametric studies. For this purpose different combinations of permeability ratio ($n = k_h/k_s$) and extent ratio ($s = r_s/r_m$) (see Fig. 2) have been adopted to investigate the effects of smear zone uncertainties on the consolidation settlement. Selected numerical parametric study results are compared with the field measurements in Fig. 10.

According to the numerical results in Fig. 10, adopting $r_s/r_w = 2$ and $k_h/k_s = 2$ causes a settlement of 4.8 m at the end of the vacuum process, while settlement is 4.0 m when $r_s/r_w = 5$ and $k_h/k_s = 5$ are adopted. This indicates that varying r_s/r_w and k_h/k_s in the range of 2–5 causes a considerable reduction in the degree of consolidation. Figure 10 shows that the smearing effect on consolidation process is more considerable in the low ranges of r_s/r_w and k_h/k_s.

The comparison of the predicted and the measured excess pore water pressure variations with time for transducer P3 located at depth 11.8 and 0.5 m away from the embankment centreline (Figs. 5 and 6) is

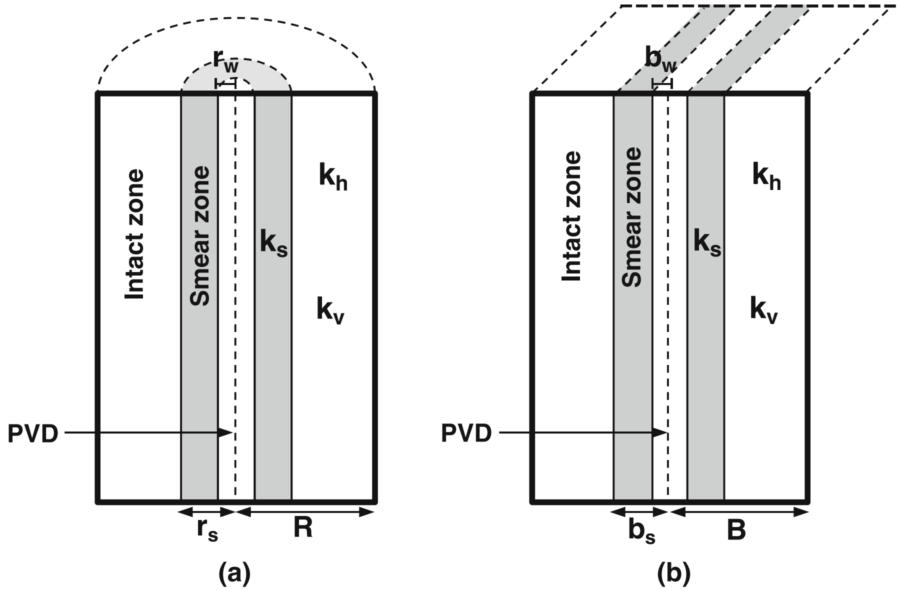

Fig. 9 Profile prefabricated vertical drain and smear zone; **a** Axisymmetric; **b** plane-strain

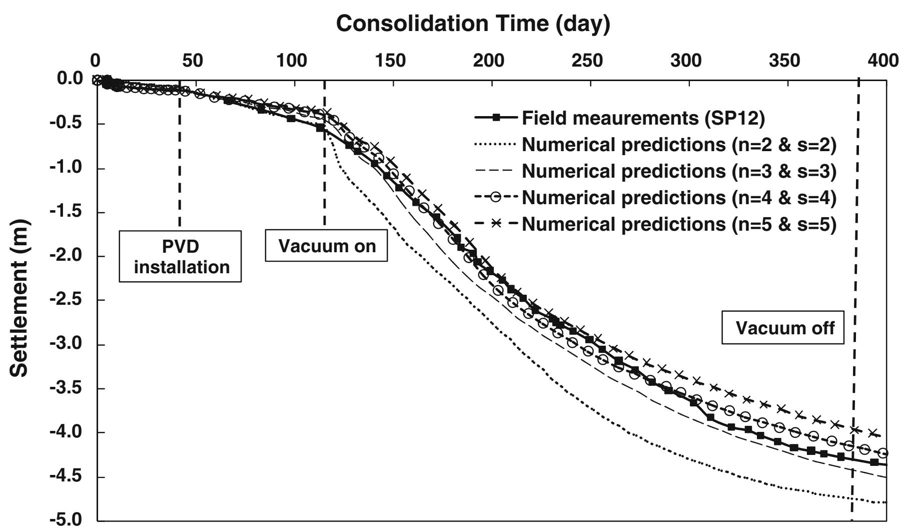

Fig. 10 Numerical parametric study results; Ballina Bypass trial embankment at SP12

illustrated in Fig. 11. According to the numerical predictions, the consolidation rate has been accelerated due to the installation of the vertical drains. It can be observed that the numerical excess pore pressure curve has experienced a sudden change of −70 kPa at the time of applying the vacuum pressure, which has been followed by an incremental trend due to the construction of embankment.

Numerical results in Fig. 11, clearly indicate that the variation of smear zone properties affect the excess pore water pressure dissipation considerably. As expected, the higher smear zone permeability leads to more accelerated excess pore water pressure dissipation. According to Fig. 11, the excess pore water pressures have been fully dissipated at the end of vacuum process considering $r_s/r_w = 2$ and $k_h/k_s = 2$, which confirms the numerical settlement predictions in Fig. 10. Adopting $r_s/r_w = 5$ and $k_h/k_s = 5$ causes the most prolonged excess pore water pressure dissipation process with the minimum settlement at the end of the vacuum process. It can be noted that the variation of r_s/r_w and k_h/k_s in the low ranges (2–3) is more critical and influences the excess pore water pressure dissipation considerably, which is in agreement with the settlement predictions given in Fig. 10. In Fig. 11, the measured excess pore water pressures

Fig. 11 Excess pore pressure variation with time for P3 at depth 11.8 m

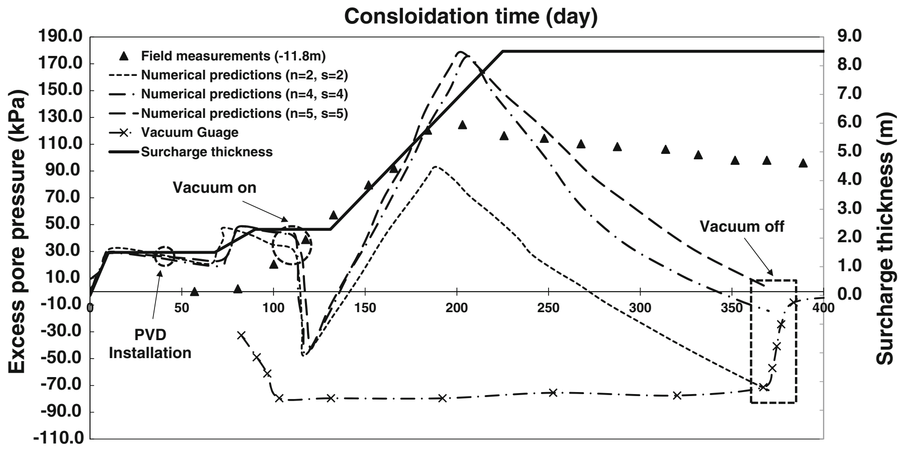

due to the staged construction of trial embankment and application of negative vacuum pressure are plotted separately, while the numerical predictions are plotted as a combined graph.

Figure 11 shows that there are disparities in the predicted excess pore water pressures and field measurements. Field measurements show that the excess pore pressure values do not dissipate immediately at the end of loading or construction, but increase or stabilise for a period before decreasing. The observed abnormal excess pore water pressure behaviour has been reported in many field studies (Conlin and Maddox 1985; Kabbaj et al. 1988; Rowe and Li 2002). Recently two main reasons have been proposed to explain that anomalous behaviour, which are called Mandel-Cryer effect and volumetric strain softening. Schiffman et al. (1969) reported that the Mandel-Cryer effect is due to the increase in total stress, which is caused by the volumetric strain compatibility. Mandel-Cryer effect is named after Mandel (1953) and Cryer (1963) based on their observations related to the abnormal excess pore water pressure generation. Cryer (1963) analysed the process of consolidation by applying an all-around pressure on a saturated porous sphere. As the surface of the sphere is free to drain, under the applied pressure, the total stress at the centre of the sphere is temporary increased because the dissipation of the excess pore water pressure at the centre is delayed. This results in increasing the excess pore water pressure for some time before the dissipation starts. In addition, the increase or delay in dissipation of the excess pore water pressure may be the result of the volumetric strain softening due to the unstable behaviour during consolidation process when the stress paths depart from the failure line. The constitutive model developed by Kimoto and Oka (2005) can capture the pore water pressure increase due to stagnation. In addition as reported by Asaoka et al. (2000), as the decay of over consolidation is much faster than degradation of the structure in clay during consolidation process, softening becomes possible with volume compression even under a considerably low stress ratio.

3.2 Case Study 2: Cumbalum Trial Embankment

A trial embankment has been constructed near Cumbalum on Pacific Highway 6.3 km north of Ballina, to provide field data for use in the design of the Ballina Bypass section of Pacific Highway upgrade in New South Wales, Australia (Kelly 2008). The embankment was constructed in 1998 by the Roads and Traffic Authority (RTA), Northern Road Services. The instrumentation layout of the embankment is shown in Fig. 12.

Vertical drains were installed at 1.35 m triangular spacings over the entire area of the embankment to approximately 22 m depth. The embankment was constructed between 1998 and 1999 to a nominal fill thickness of 4.5 m. Later site investigations through the trial embankment showed that approximately 5 m of fill had actually been placed. The embankment was then allowed to consolidate for about 4.5 years. Measurements at the location of Settlement Plate 9 (SP9) are used for the numerical verification and the parametric study. The subsoil profile consists of

Fig. 12 Layout of the Cumbalum trial embankment (after RTA, 2000)

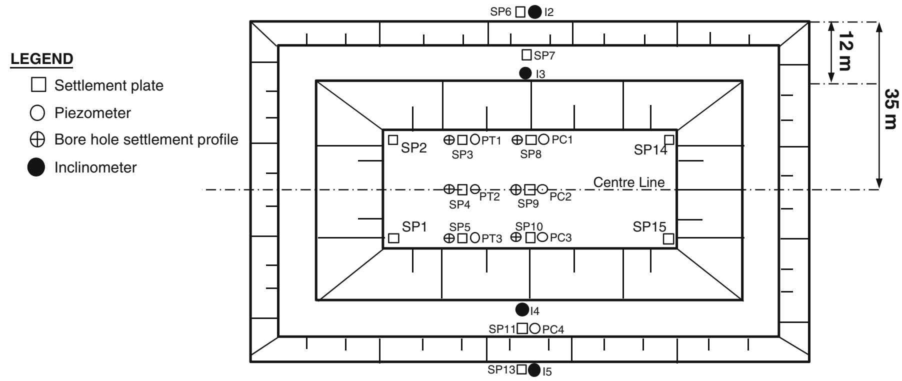

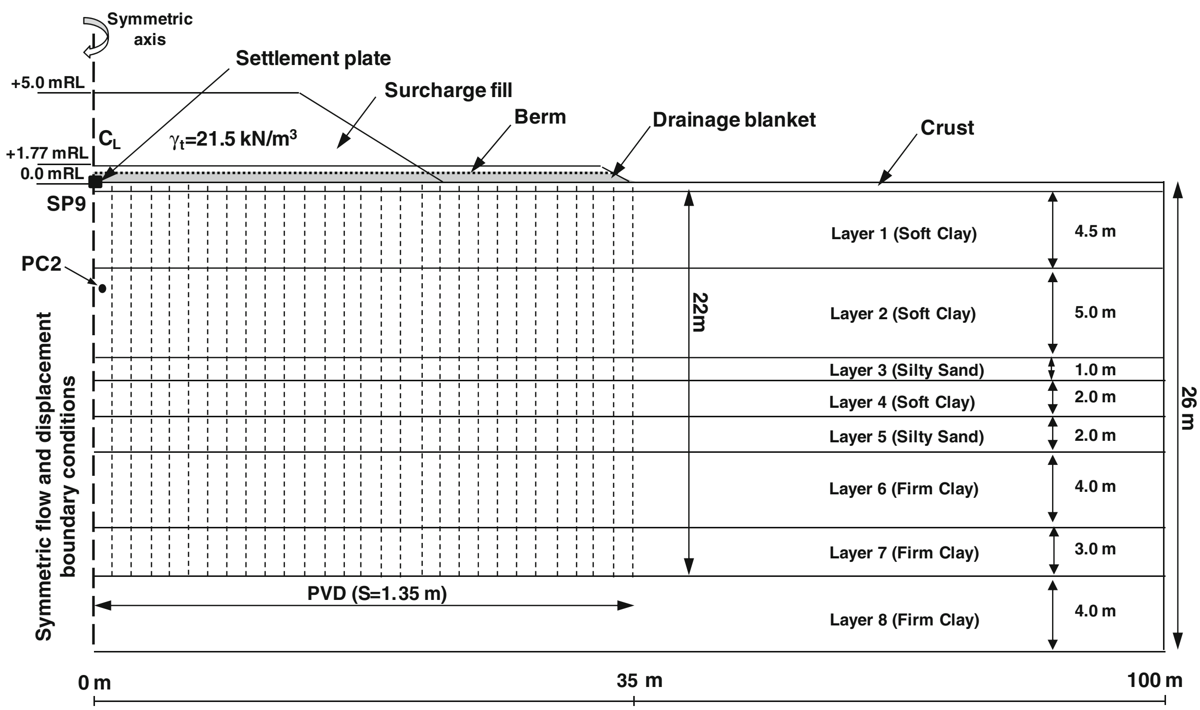

Fig. 13 Cross section of the Cumbalum trial embankment and subsoil profile

lightly consolidated soft clay deposits from ground surface level to the depth of 10 m with the average OCR of 1.75. According to the site investigation results, 2 m of soft clay is located at the depth of 12 m with the OCR of 1.3, which is surrounded with two silty sand lenses. The soil deposit between depth of 15 and 22 m has the average OCR of 2.2 and is categorised as firm clay. Figure 13 presents the cross-section of the embankment and subsoil profile at SP9. The MCC mode is adopted to model the soil behaviour in both the intact region and the smear zone, while the Mohr–Coulomb criteria elastic-perfectly plastic model is applied for the embankment simulation. The construction history of the embankment is shown in Fig. 14 and the adopted properties for subsoil layers are summarised in Table 3.

The finite difference mesh used for 2D plane-strain numerical simulation is illustrated in Fig. 15. The vertical drains were modelled by fixing the pore pressure to the hydrostatic pressure from the top to the bottom of the drain. A constant reduced permeability was assigned to the vertical drain surrounded area in

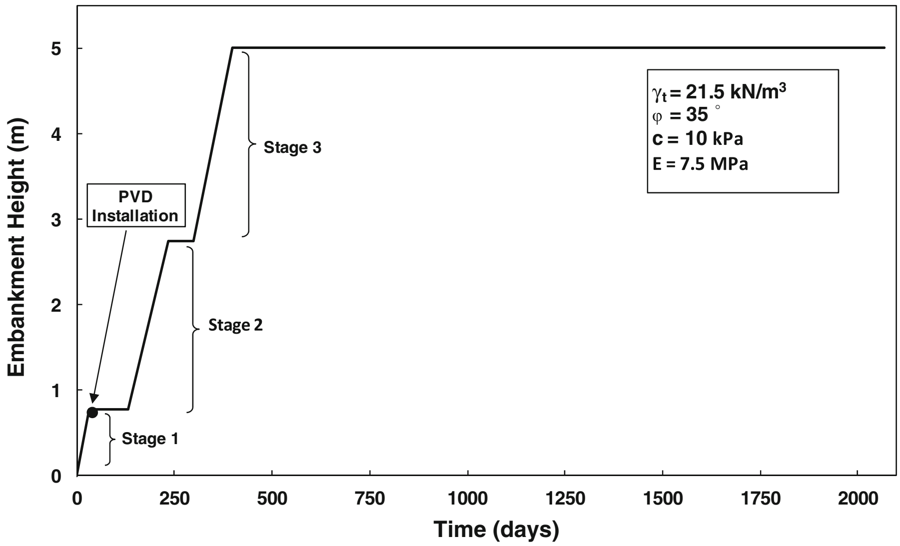

Fig. 14 Construction history of Cumbalum trial embankment

each layer to simulate the smear zone (see Fig. 15). The vertical drain system was converted into an equivalent parallel drain wall adopting Eq. (4).

FLAC code has been applied to conduct the parametric studies varying the k_h/k_s and r_s/r_m from 2 to 6. The effects of smear zone uncertainties on consolidation rate are illustrated in Fig. 16, plotting the numerical predictions for the selected combinations of k_h/k_s and r_s/r_m. It can be observed that the variation of smear zone permeability and extent have a substantial influence on the settlement rate. Figure 16 shows that the settlement has increased from 2.3 to 3.0 m varying k_h/k_s and r_s/r_m from 6 to 2 after 1,900 days of consolidation. According to the plotted graphs in Fig. 16, the settlement curve corresponding to the case with the smear zone characteristics of $k_h/k_s = 5$ and $r_s/r_m = 5$ is in a good agreement with the field measurement. However, it is not possible to verify this agreement by observation at the initial stages of trial embankment construction and a systematic back calculation procedure is required.

Figure 17 illustrates the predicted and measured values of excess pore water pressure at the location of PC2 at the depth of 5.8 m (Figs. 12 and 13). It can be observed that the excess pore water pressure curves for the numerical predictions and the field measurements follow a similar pattern. The pore pressures increased during the fill placement *a*t each stage of the embankment construction and then dissipated slightly. The maximum excess pore water pressure for each case occurred at the end of embankment construction process, similar to the field observations reported by Kabbaj et al. (1988) and Leroueil (1997). Figure 17 shows that the maximum excess pore water pressure of 120 kPa occurs at the end of embankment construction process adopting $k_h/k_s = 6$ and $r_s/r_m = 6$. It can be noted that the lower k_h/k_s and r_s/r_m values cause a sharper dissipation of excess pore water pressure. For example, 90 % of the excess pore water pressure has been dissipated after 1,900 days adopting $k_h/k_s = 2$ and $r_s/r_m = 2$, while this dissipation is 70 % for the case with $k_h/k_s = 6$ and $r_s/r_m = 6$.

According to Fig. 17, there are some discrepancies between measured and predicted excess pore water pressures. Compared to the field values, predicted excess pore pressures are larger at the end of the embankment construction process, and in better agreement when consolidation process is completed. This discrepancy can be attributed to numerous factors such as the uncertainty of soil properties, the effect of smear characteristics, inaccurate assumptions of soil behaviour and an improper conversion of axisymmetric conditions to plane strain (2D) analysis of multiple drains. Furthermore, it can be noted that the smear effect on consolidation process is more significant on Cumbalum trial embankment comparing with Ballina

Table 3 Adopted properties for subsoil layers for Cumbalum trial embankment near SP9

Depth: m	λ	κ	e_0	γ_s (kN/m^3)	k_h (10^{-10} m/s)	k_v (10^{-10} m/s)	OCR
0.0–0.5	0.7	0.042	2.2	17.5	2.04	1.02	3.0
0.5–5.0	0.84	0.118	2.87	15.0	1.71	0.85	2.0
5.0–10.0	0.95	0.134	3.4	14.0	1.71	0.85	1.5
10.0–11.0	0.125	0.031	2.61	18.0	1,260	630	3.0
11.0–13.0	0.61	0.087	3.0	15.0	1.74	0.87	1.3
13.0–15.0	0.125	0.031	2.61	18.0	1,740	870	3.0
15.0–19.0	0.47	0.067	2.08	17.0	2.94	1.5	1.3
19.0–22.0	0.335	0.047	2.08	20.0	2.94	1.5	3.5
22.0–26.0	0.335	0.047	2.08	20.0	2.94	1.5	2.5

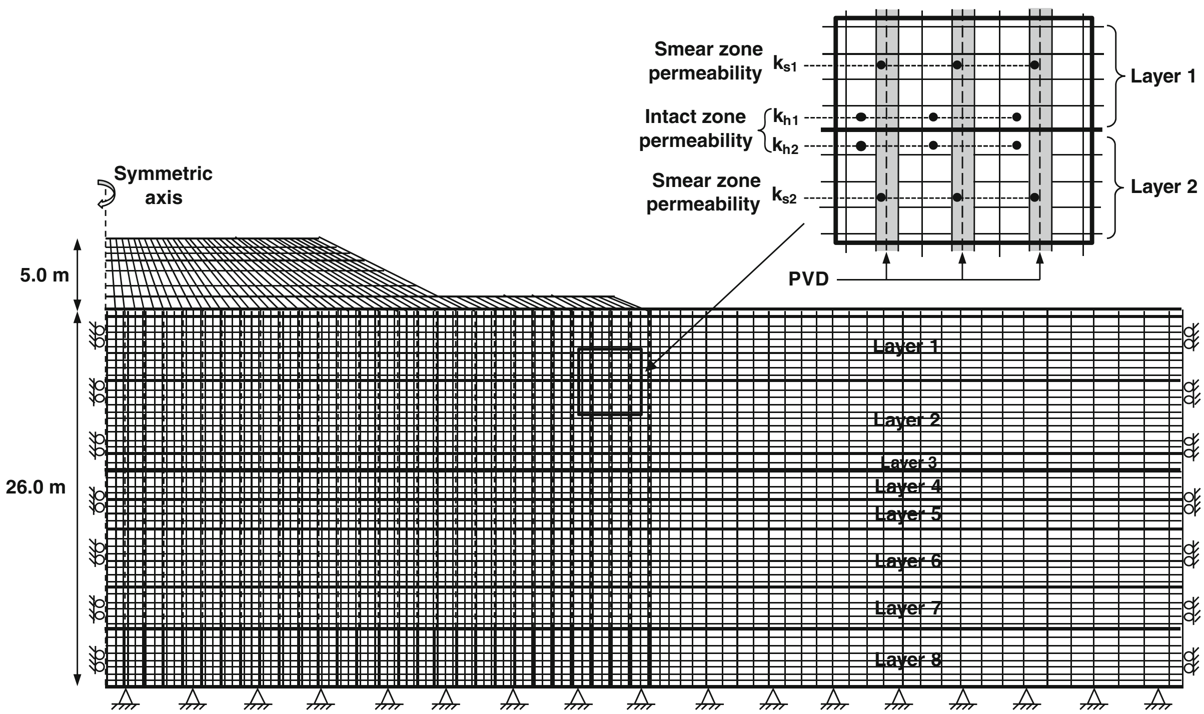

Fig. 15 Finite-difference mesh for the plane-strain analysis of Cumbalum trial embankment

Bypass trial embankment (similar clays were encountered), which can be result of using different wick drains, different end plate sizes and loss of drain efficiency due to the clogging of the drains as the consolidation period is much longer in Cumbalum project. Furthermore, in this study, effects of possible soil texture or cementation/structure degradation in the clay under the applied loads have been ignored (Nguyen et al. 2014; Fatahi et al. 2012b).

3.3 Case Study 3: Sunshine Trial Embankment

A fully instrumented Sunshine trial embankment has been selected as the third case study to verify the numerical analysis adopting FLAC code and conduct the parametric study. The trial embankment was constructed and monitored by the Queensland Department of Transport (1992). The subsoil conditions are relatively uniform throughout the site, consisting of

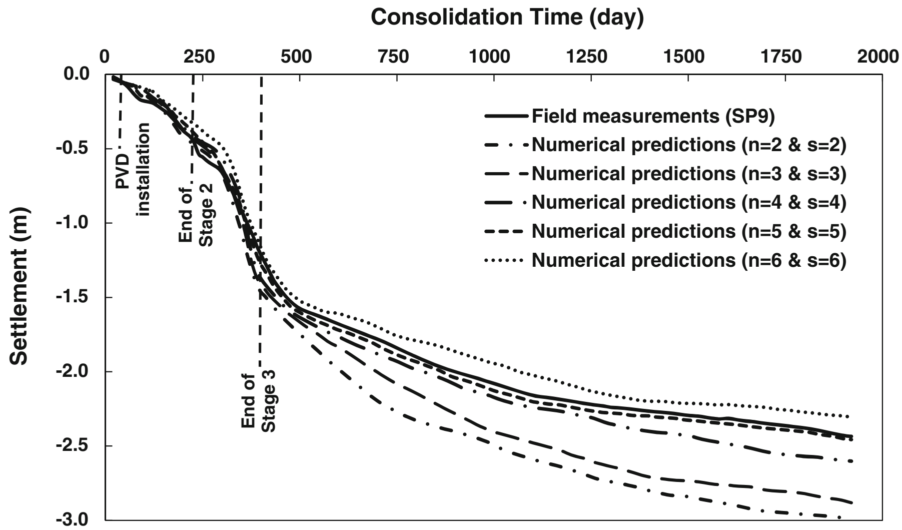

Fig. 16 Numerical parametric study results; Cumbalum trial embankment at SP9

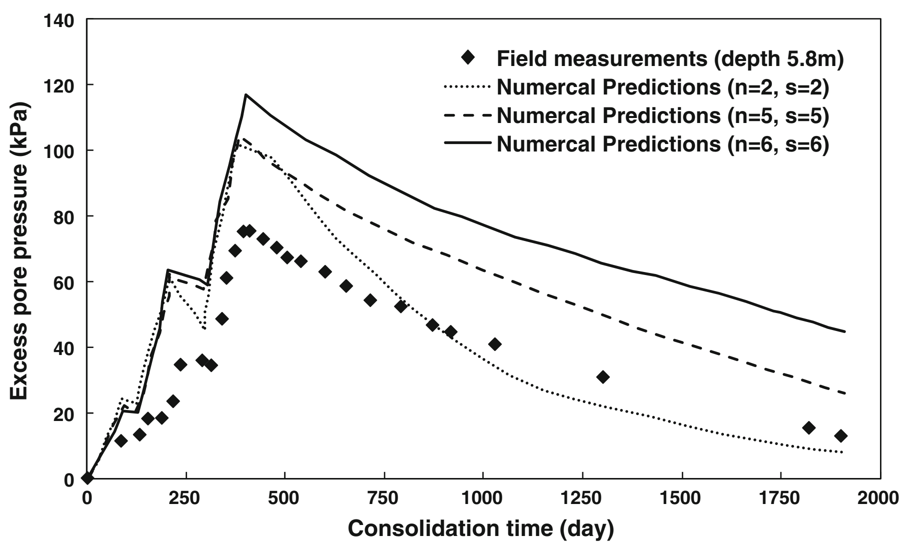

Fig. 17 Excess pore pressure variation with time for PC2 at depth 5.8 m

silty/sandy clay approximately 11 m thick, overlying a layer of dense sand approximately 6 m thick. Among the available sections in this trial project, the section with the vertical drain spacing of 2 m has been selected. PVDs (Nylex Flodrain, 100 × 4 mm^2) were installed in a triangular pattern. A working platform 0.65 m thick (500 mm thick drainage layer composed of 7 mm size gravel, plus 150 mm of selected fill) was placed on the natural ground surface for the construction traffic access. PVDs were installed from the working platform to the depth of 11 m. The embankment was constructed in stages using a loosely compacted granular material ($\gamma_s = 19$ kN/m^3) up to a height of 2.3 m. A detailed cross section of the embankment with a selected instrumentation point is shown in Fig. 18. Further details of this project can be found in Sathananthan et al. (2008) and Queensland Department of Transport (1992). Figure 19 illustrates the embankment construction history.

The MCC constitutive model has been selected to model the consolidation behaviour of the subsoil profile applying finite difference code FLAC. The Mohr–Coulomb model has been utilised to simulate the silty sand embankment. The over consolidation ratio of 1.6 has been adopted in this study and the horizontal permeability of the intact zone (k_h) was

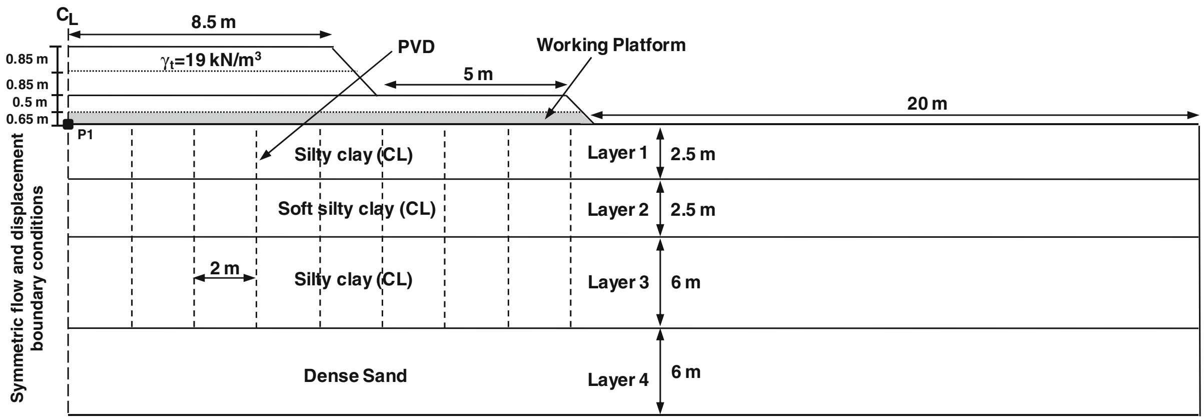

Fig. 18 Cross section of the sunshine trial embankment and ground

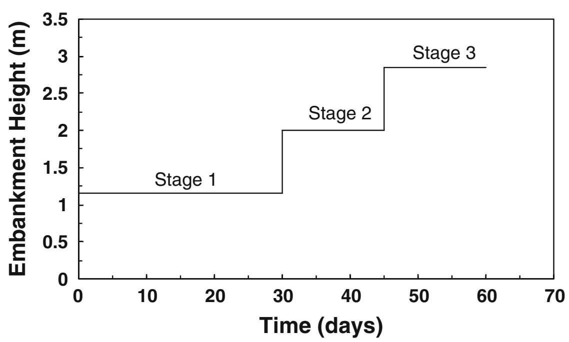

Fig. 19 Construction history of the sunshine trial embankment

considered approximately twice of the vertical permeability (k_v). It is assumed that vertical and horizontal permeability values in the smear zone are the same. The equivalent plane-strain permeability is estimated based on Eq. (4). The properties of subsurface ground profile and embankment material are summarised in Tables 4 and 5, respectively. The discretised finite difference mesh is shown in Fig. 20. Because of symmetry, it was sufficient to consider one half of the embankment for the numerical analysis, and a finer mesh was employed to simulate the smear zone.

The developed numerical code has been verified comparing FLAC results with the field data. In addition, the proposed back calculation scheme was used adopting different combinations of smear zone properties to conduct a systematic parametric study and results are reported in Fig. 21. According to Fig. 21, 1.0 m of settlement is observed after 90 days of consolidation for the case with $k_h/k_s = 2$ and $r_s/r_m = 3$, while adopting $k_h/k_s = 6$ and $r_s/r_m = 3$ can cause a reduction of 0.3 m in the consolidation settlement after the same elapsed time, demonstrating that the variation of smear zone properties can considerably affect the consolidation rate. Figure 21 indicates that, the case with $k_h/k_s = 4$ and $r_s/r_m = 3$ provides the best fit with the field measurements. It can be observed that the smear zone permeability ratio is not a key factor in the first stage of embankment construction which lasted 30 days. By increasing the height of the embankment from 1.15 m to 2.85 m, the variations in permeability ratio (k_h/k_s) play a more significant role in the predicted settlement curve. It is clearly observed that the smear zone uncertainties can affect the consolidation time considerably particularly in higher degree of consolidation.

4 Minimum Required Degree of Consolidation and Discussion

FLAC code was used to estimate the primary consolidation settlement for each case study under the embankment surcharge adopting the MCC soil properties that are reported in Tables 2, 3 and 4. The field settlements at the end of preloading process are extracted from Figs. 10, 16 and 21. The corresponding degree of consolidation is determined using Eq. (7). Results are summarised in Table 6.

$$U\% = \frac{s_t}{s_f} \times 100 \tag{7}$$

where U % is the degree of consolidation at time t, s_t is the field settlement at time t, and s_f is the predicted final primary consolidation settlement.

Table 4 Adopted properties for the numerical simulation (after Sathananthan et al. 2008)

Layer	Soil type	M	λ	κ	ν	e_0	γ_s (kN/m^3)	k_{hp} (10^{-9} m/s)	k_h/k_v
1	Silty clay	1.20	0.494	0.0494	0.3	1.6	16.4	9.72	2
2	Soft Silty clay	1.20	2.016	0.2016	0.3	2.2	13.7	0.34	2
3	Silty clay	1.18	0.532	0.0532	0.3	1.8	15.9	0.42	2

M is the slope of the critical state line; λ and κ are slopes of the specific volume versus $ln(p')$ curves for compression and swelling, respectively, where p' is the mean effective stress; ν is the Poisson's ratio; e_0 is the initial void ratio; and k_{hp} is the permeability of intact zone in the plane-strain condition

Table 5 Applied properties for sand layer (after Sathananthan et al. 2008)

Layer	Soil type	c' (kPa)	φ'(deg)	*E* (MPa)	ν
4	Dense sand	13.5	35	7.5	0.3

It should be noted that in this study as a simplifying assumption, the effects of soil creep during the excess pore water pressure dissipation have been ignored. It should be considered that the key purpose of this study is establishing the minimum required degree of consolidation to back-calculate smear zone properties reliably. Thus, it is more practical to adopt conventional consolidation theory to predict the settlement at the end of primary consolidation. However as reported by Yin and Graham (1989), Le et al. (2012) and Fatahi et al. (2013), adopting elasto-viscoplastic soil model, the soil creep due to the drainage of pore fluid in micropores, or due to the structural viscosity of pore fluids, can be simulated explicitly during the excess pore water pressure dissipation.

Effects of smear zone properties on the consolidation rate are summarised in Table 7. It can be observed that smear zone characteristics considerably affect the preloading settlement rate, which should be considered in practical designs. It can be observed that varying r_s/r_w and k_h/k_s from 2 to 5 causes a reduction of 17 % in the degree of consolidation from 92 to 75 % for the Ballina Bypass trial embankment. Table 7 shows that changing k_h/k_s and r_s/r_m from 6 to 2 can increase the degree of consolidation by 20 % for the Cumbalum trial embankment. In Sunshine trial embankment, increasing the permeability ratio (k_h/k_s) from 2 to 6, while considering a constant extent ratio (r_s/r_m) of 3, can reduce the degree of consolidation from 57 to 40 %.

According to Figs 10, 16 and 21, it is not possible to employ the observational approach to estimate reliable smear zone properties in the early stages of the trial embankment construction resulting in the settlement curves having the best agreement with the field measurements. Therefore, a systematic procedure is

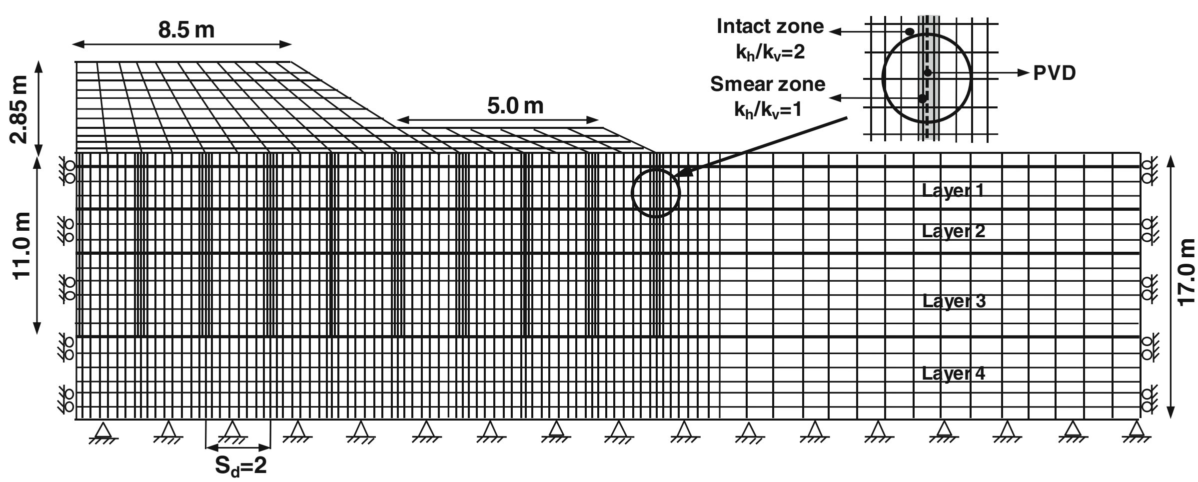

Fig. 20 Finite-difference mesh of embankment for plane-strain analysis at sunshine motorway

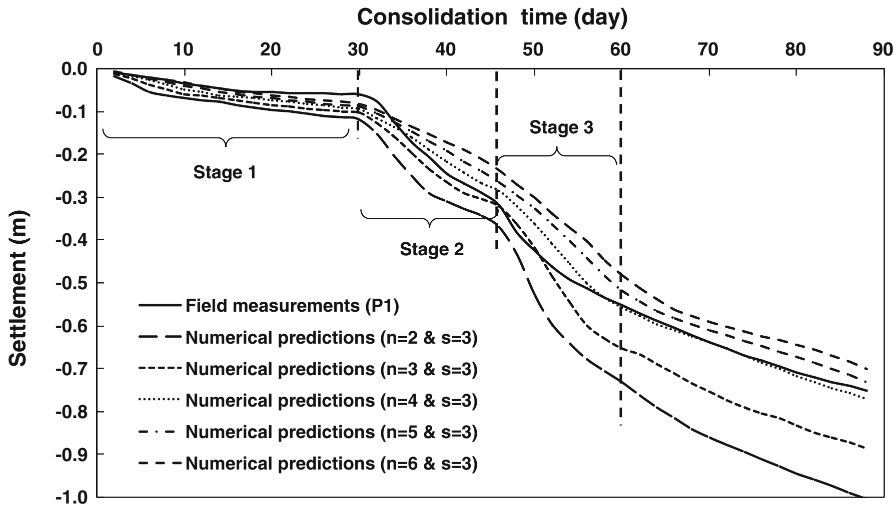

Fig. 21 Numerical parametric study results; sunshine trial embankment at P1

Table 6 Primary consolidation settlement

Case study	Ballina bypass at SP12	Cumbalum at SP9	Sunshine at P1
Primary settlement (*m*)	5.2	3.3	1.75
Field settlement at the end of preloading (*m*)	4.4	2.45	0.75
Preloading time (day)	400	2,000	90
Degree of consolidation at the end of preloading (%)	85 %	75 %	40 %

Table 7 Effect of smear zone characteristics variation on consolidation settlement rate

Ballina bypass trial embankment					
n (k_h/k_s)	2	3	4	5	
s (r_s/r_m)	2	3	4	5	
S_p (m)	4.79	4.50	4.24	3.9	
U % (400 days)	92 %	87 %	81 %	75 %	
Cumbalum trial embankment					
n (k_h/k_s)	2	3	4	5	6
s (r_s/r_m)	2	3	4	5	6
S_p (m)	3.0	2.88	2.6	2.45	2.3
U % (2,000 days)	90 %	87 %	78 %	74 %	70 %
Sunshine trial embankment					
n (k_h/k_s)	2	3	4	5	6
s (r_s/r_m)	3	3	3	3	3
S_p (m)	1.00	0.89	0.77	0.73	0.70
U % (90 days)	57 %	51 %	44 %	42 %	40 %

S_p is the predicted settlement at the end of preloading process and U % is the corresponding degree of consolidation

required to determine the existing error between the field measurements and numerical predictions adopting specific smear zone properties at every degree of consolidation and find the optimum combination of r_s/r_w and k_h/k_s. For this purpose, the third stage of the proposed back calculation procedure is used to determine the optimum combination of r_s/r_w and k_h/k_s, resulting in the best predictions by calculating the accumulative error at each stage of the consolidation process. The following equation is used to determine a normalised accumulative error:

$$(E_t)_n = \sum_{i=1}^{n} \frac{(S_t)_i - (S_{tp})_i}{N \times S_f} \quad (8)$$

where, E_t is the normalised accumulative error at time t, n is the observation point number, N is the total number of observation points, S_t is the field settlement at time t, S_{tp} is the predicted settlement at time t, and S_f is the final primary consolidation settlement.

Figure 22 illustrates the normalised accumulative error against the degree of consolidation for three case studies for different smear zone properties. In each case study, the best predicted smear zone properties ($s = r_s/r_w$ and $n = k_h/k_s$), belong to the case with the minimum final accumulative error. The final accumulative errors for different combinations of n and s are tabulated in Table 8. The highlighted cells are the smear zone properties resulting in the minimum final

Fig. 22 Normalised accumulative error versus degree of consolidation for different smear zone properties; **a** Ballina bypass trial embankment at SP12; **b** cumbalum trial embankment at SP9; **c** sunshine trial embankment at P1

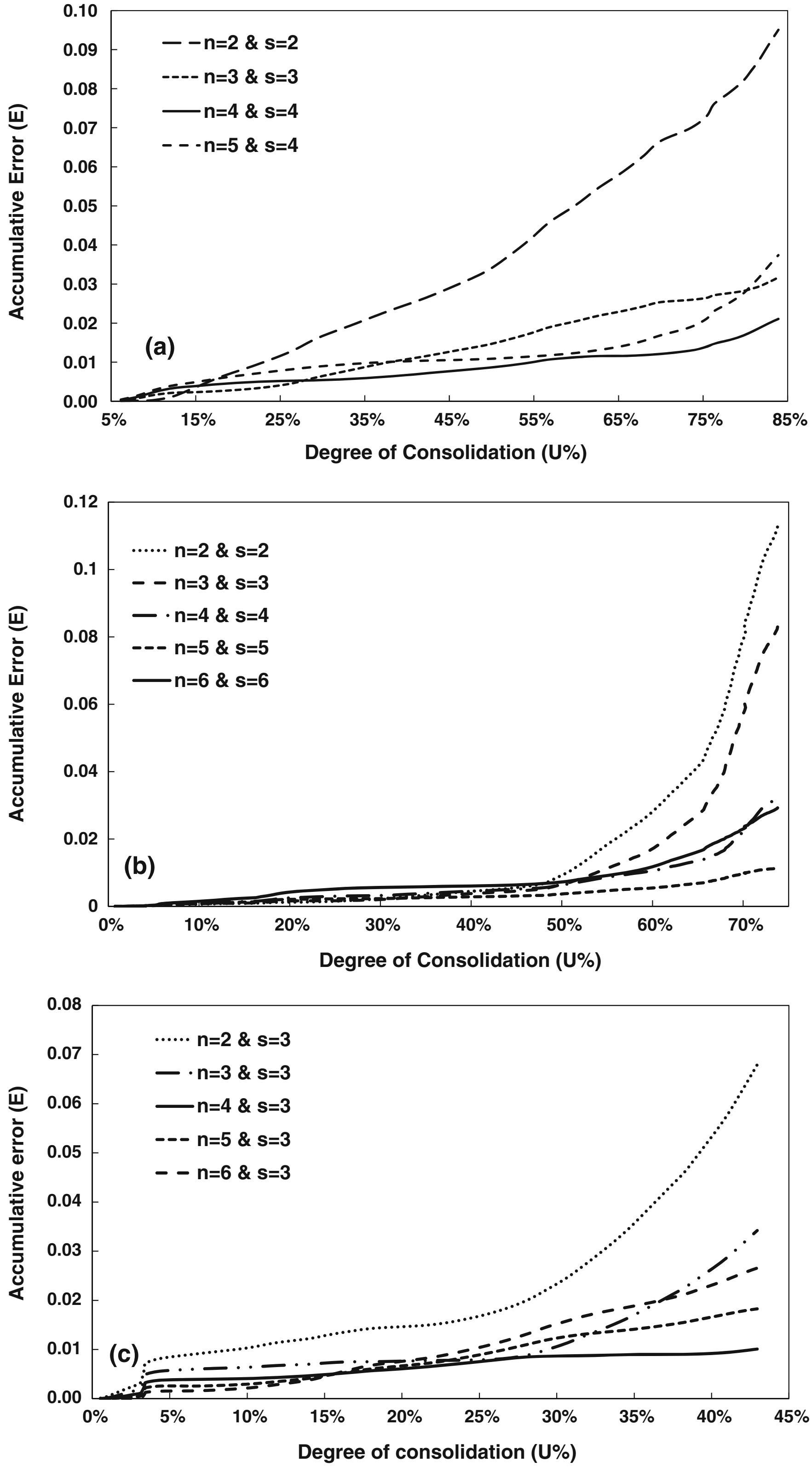

Table 8 Effect of smear zone characteristics variation on consolidation settlement rate

Ballina bypass trial embankment					
n (k_h/k_s)	2	3	4	5	
s (r_s/r_m)	2	3	4	5	
E_f	0.095	0.032	0.021	0.037	
Cumbalum trial embankment					
n (k_h/k_s)	2	3	4	5	6
s (r_s/r_m)	2	3	4	5	6
E_f	0.113	0.083	0.032	0.011	0.029
Sunshine trial embankment					
n (k_h/k_s)	2	3	4	5	6
s (r_s/r_m)	3	3	3	3	3
E_f	0.068	0.034	0.010	0.018	0.027

E_f is the final accumulative error

accumulative error and the corresponding curve has the best fit with the field measurements, which can be reported as the best predicted smear zone characteristics. According to the graphs in Fig. 22, estimation of the smear zone characteristics at the very early stages of the embankment construction is a challenging task and accurate values cannot be well predicted.

To determine the minimum required degree of consolidation (minimum waiting time) resulting in the most accurate r_s/r_w and k_h/k_s values corresponding to the minimum accumulative errors at every degree of consolidation have been defined and the corresponding final accumulative error for each case against the degree of consolidation are plotted in Figs 23a–c. The minimum required degree of consolidation and corresponding time belong to the first point with the minimum accumulative error. The predicted smear zone properties (r_s/r_m and k_h/k_s) at that point can be reported as the reliable values for the practical design purposes.

Figure 23a shows that for the Ballina Bypass trial embankment, there is no change in the value of the final accumulative error after 26 % degree of consolidation, corresponding to the case with the smear zone properties of $r_s/r_w = 4$ and $k_h/k_s = 4$. Therefore, reliable smear zone properties predictions can be obtained after 26 % degree of consolidation. According to the plotted graph for the Cumbalum trial embankment in Fig. 23b, 33 % degree of consolidation can be reported as the minimum period that needs to be considered to estimate the smear zone characteristics accurately. Figure 23c illustrates that the smear zone properties can be well predicted for the Sunshine trial embankment when 16 % degree of consolidation is obtained. Referring to Fig. 23c, the final accumulative error for Sunshine trial embankment has a constant and minimum value of 0.01 after 16 % degree of consolidation, which belongs to the case with $k_h/k_s = 4$ and $r_s/r_m = 3$.

By looking at the results obtained from the mentioned case studies, the construction of trial embankment with field measurements is recommended as a practical solution to estimate the smear zone properties as accurate as possible, and the minimum required waiting time should be designed to obtain at least 33 % degree of consolidation. Thus, the following steps are recommended to predict the smear zone permeability and extent; (1) construction of trial embankment; (2) numerical determination of the final settlement; (3) back calculation of smear zone properties employing the proposed back calculation procedure, when at least 33 % of predicted final settlement is obtained (i.e. after achieving 33 % degree of consolidation).

5 Conclusions

The current literature proposes a wide range of smear zone characteristics to be used in the practical design and no comprehensive method has been proposed so far to estimate the smear zone properties accurately. Construction of a trial embankment and corresponding field measurements have been used by a number of researchers to determine the feasibility of preloading with vertical drains and to estimate the smear zone properties using the back calculation analysis. It has always been a considerable challenge to decide how long the trial embankment should be in place to obtain accurate back calculated results and this has both cost and construction time consequences. Estimation of the smear zone permeability and extent in the early stages of the trial embankment construction can convert this method to a very practical, accurate and cost effective approach. In this paper, a back calculation method is combined with the numerical analysis to determine the minimum required waiting time after construction of a trial embankment to obtain reliable smear zone characteristics.

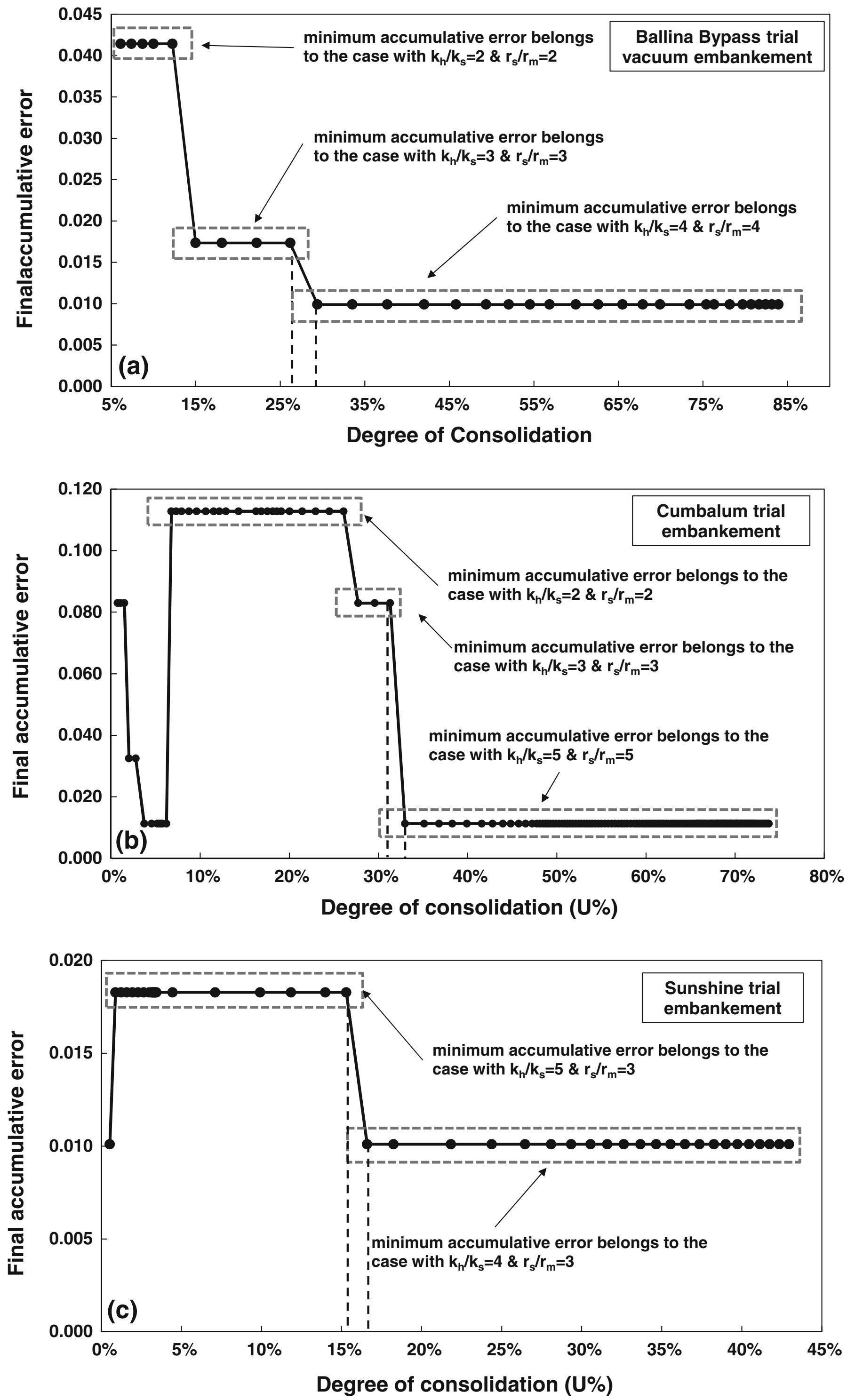

Fig. 23 Total accumulative error (for the smear zone properties resulting in minimum accumulative error) versus degree of consolidation; **a** Ballina bypass trial embankment at SP12; **b** cumbalum trial embankment at SP9; **c** sunshine trial embankment at P1

In this study, a finite difference explicit numerical code has been developed in plane-strain condition employing FLAC 2D software to investigate the effect of smear zone characteristics on the performance of the soft clay foundations beneath embankments stabilised with vertical drains. New subroutines have been embedded in the FLAC code using the built-in programming language FISH (FLACish) to facilitate the simulation process and conduct the parametric study appropriately. The MCC model was adopted to simulate the constitutive behaviour of the soft soil and Biot theory of consolidation was considered for the formulation of coupled fluid-deformation mechanisms. A back calculation procedure is proposed to conduct systematic parametric studies to estimate the smear zone properties precisely, comparing the numerical results with the field measurements and determine the available error. The proposed back calculation procedure (Fig. 4) was applied to predict the minimum required degree of consolidation (i.e. the minimum waiting time after trial embankment construction), obtaining reliable smear zone properties. Three trial embankments stabilised with vertical drains in Australia, including Ballina Bypass, Cumbalum and Sunshine trial embankments, were simulated to verify the developed FLAC code and conduct the systematic parametric study adopting the back calculation procedure.

The parametric study results clearly indicate that the properties of the smear zone have key roles on the required consolidation time to achieve a certain soil strength and stiffness, satisfying both bearing capacity and settlement design criteria. Therefore, an accurate estimation of the properties of smear zone based on the soil type and the installation method is vital for the ground improvement projects adopting PVD assisted preloading. The smear zone properties have been well-predicted for all simulated trial embankments applying the developed FLAC code adopting the proposed back calculation procedure, which indicated the validity of the numerical code and the back calculation procedure.

The application of the numerical analysis in conjunction with the proposed back calculation procedure conducting a systematic parametric study is recommended to designers as a practical solution to predict the smear zone properties precisely adopting monitoring field measurements. According to the results obtained from case studies, the properties of the smear zone can be well back calculated after achieving at least 33 % degree of consolidation. It should be noted that the proposed minimum waiting time has been obtained through the simulation of three case studies (one vacuum preloading and two PVD assisted preloading with surcharge) and further verifications would be helpful to strengthen this conclusion.

Acknowledgments This research has been supported by the Australian Research Council (LP0991643) and Menard-Bachy Pty Ltd. The Authors acknowledge their supports. Also, the authors wish to thank the Roads and Maritime Services (RMS) of NSW for providing the field investigation and monitoring results.

References

Abuel-Naga HM, Bergado DT, Chaiprakaikeow S (2006) Innovative thermal technique for enhancing the performance of prefabricated vertical drain during the preloading process. Geotext Geomembr 24(6):359–370

Akagi T (1976) Effect of displacement type sand drains on strength and compressibility of soft clays. PhD Thesis University of Tokyo

Almedia MSS, Danzigner FAB, Almdia MCL, Carvalho SR, Martins IS (1993) Performance of an embankment built on a soft disturbed clay. In: 3rd international conference case histories in Geotechnical Engineering, Missouri, pp 351–356

Asaoka A, Nakano M, Noda T, Kaneda K (2000) Delayed compression/consolidation of natural clay due to degradation of soil structure. Soils Found 40(3):75–85

Balasubramaniam AS, Huang M, Bolton M, Oh EYN, Bergado DT, Phienwe NJ (2007) Interpretation and analysis of test embankments in soft clays with and without ground improvement. Paper presented at the sixteenth southeast Asian geotechnical conference

Barron RA (1948) Consolidation of fine-grained soils by drain wells. Trans Am Soc Civil Eng 113(1):718–742

Basu D, Prezzi M (2007) Effect of the smear and transition zones around prefabricated vertical drains installed in a triangular pattern on the rate of soil consolidation. Int J Geomech 7(1):34–43

Basu D, Basu P, Prezzi M (2006) Analytical solutions for consolidation aided by vertical drains. Geomech Geoeng 1(1):63–71

Bergado DT, Mukherjeea K, Alfaroa MC, Balasubramaniama AS (1993) Prediction of vertical-band-drain performance by the finite-element method. Geotext Geomembr 12(6): 567–586

Bergado DT, Chai JC, Miura N, Balasubramaniam AS (1998) PVD improvement of soft Bangkok clay with combined vacuum and reduced sand embankment preloading. Geotech Eng 29(1):95–122

Bhosle P, Vaishampayan VV (2009) Case study for ground improvement using PVD with preloading for coal and iron ore stack yard. Paper presented at the annual conference of the Indian Geotechnical Society (IGC), Guntur, India

Biot MA (1941) General theory of three-dimensional consolidation. Appl Phys 12:155–164

Bo MW, Chu J, Choa V (2003) Soil improvement: prefabricated vertical drain techniques. Thompson, Singapore

Chai J, Miura N (1999) Investigation of factors affecting vertical drain behavior. J Geotech Geoenviron Eng 125(3):216–226

Conlin BH, Maddox WP (1985) An assessment of the behaviour of foundation clay at Tarsiut N-44 Caisson retained island. In: 17th offshore technology conference, Houston, Texas, pp 379–388

Cryer CW (1963) A comparison of the three dimensional consolidation theories of Biot and Terzaghi. Q J Mech Appl Math 16(4):401–412

Eriksson U, Hansbo S, Torstensson BA (2000) Soil improvement at Stockholm-Arlanda airport. Ground Improv 4(2):73–80

Fatahi B, Khabbaz H, Indraratna B (2009) Parametric studies on bioengineering effects of tree root-based suction on ground behaviour. Ecol Eng 35(10):1415–1426

Fatahi B, Khabbaz H, Indraratna B (2010) Bioengineering ground improvement considering root water uptake model. Ecol Eng 36(2):222–229

Fatahi B, Basack S, Premananda S, Khabbaz H (2012a) Settlement prediction and back analysis of Young's modulus and dilation angle of stone columns. Aust J Civil Eng 10(1):67–78

Fatahi B, Khabbaz H, Fatahi B (2012b) Mechanical characteristics of soft clay treated with fibre and cement. Geosynth Int 19(3):252–262

Fatahi B, Le TM, Le MQ, Khabbaz H (2013) Soil creep effects on ground lateral deformation and pore water pressure under embankments. Geomech Geoeng 8(2):107–124

Ghandeharioon A, Indraratna B, Rujikiatkamjorn C (2010) Analysis of soil disturbance associated with mandrel-driven prefabricated vertical drains using an elliptical cavity expansion theory. Int J Geomech 10(2):53–64

Ghandeharioon A, Indraratna B, Rujikiatkamjorn C (2012) Laboratory and finite-element investigation of soil disturbance associated with the installation of mandrel-driven prefabricated vertical drains. J Geotech Geoenviron Eng 138(3):295–308

Hansbo S (1994) Foundation engineering. Elsevier Science B. V, Amsterdam

Hansbo S (1997) Practical aspects of vertical drain design. In: 14th international conference on soil mechanics and foundation engineering, Hamburg, pp 1749–1752

Hansbo S, Jamiolkowski M, Kok L (1981) Consolidation by vertical drains. Geotechnique 31:45–66

Hawlader BC, Muhunthan B (2002) Numerical study of the factors affecting the consolidation of clay with vertical drains. Geotext Geomembr 20(4):213–239

Hird CC, Moseley VJ (2000) Model study of seepage in smear zones around vertical drains in layered soil. Géotechnique 50(1):89–97

Hird CC, Pyrah IC, Russell D, Ciuicioglu F (1995) Modelling the effect of vertical drains in two-dimensional finite element analyses of embankments on soft ground. Can Geotech J 32(5):795–807

Hokmabadi AS, Fatahi B, Samali B (2014a) Assessment of soil–pile–structure interaction influencing seismic response of mid-rise buildings sitting on floating pile foundations. Comput Geotech 55(1):172–186

Hokmabadi AS, Fatahi B, Samali B (2014b) Seismic response of mid-rise buildings on shallow and end-bearing pile foundations in soft soils. Soils Found 54(3):345–363

Indraratna B, Redana IW (1997) Plane-strain modelling of smear effects associated with vertical drains. J Geotechn Geoenviron Eng 123(5):474–478

Indraratna B, Redana IW (1998) Laboratory determination of smear zone due to vertical drain installation. J Geotech Geoenviron Eng 124(2):180–184

Indraratna B, Redana IW (2000) Numerical modelling of vertical drains with smear and well resistance installed in soft clay. Can Geotech J 37(1):132–145

Indraratna B, Rujikiatkamjorn C, Balasubramaniam C, Wijeyakulasuriya V (2005a) Predictions and observations of soft clay foundations stabilized with geisynthetic drains and vacuum surcharge. In: Indraranata B, Chu J (eds) Ground improvement: case histories, vol 3. Elsevier, London, pp 199–230

Indraratna B, Sathananthan I, Rujikiatkamjorn C, Balasubramaniam AS (2005b) Analytical and numerical modelling of soft soil stabilized by prefabricated vertical drains incorporating vacuum preloading. Int J Geomech 5(2): 114–124

Indraratna B, Rujikiatkamjorn C, Sathananthan I, Shahin M, Khabbaz H (2005c) Analytical and numerical solutions for soft clay consolidation using geosynthetic vertical drains with special reference to embankments. Paper presented at the the fifth international geotechnical engineering conference, Cairo, Egypt

Indraratna B, Rujikiatkamjorn C, Ameratunga J, Boyle P (2011) Performance and prediction of vacuum combined surcharge consolidation at Port of Brisbane. Geotech Geoenviron Eng 137(11):1009–1018

Jamiolkowski M, Lancellotta R, Wolski W (1983) Precompression and speeding up consolidation. In: 8th European conference on soil mechanics and foundation engineering, Helsinki, Balkema, Rotterdam, the Netherlands, pp 1201–1226, 23–26 May 1983

Kabbaj M, Tavenas F, Leroueil S (1988) In situ and laboratory stress-strain relationships. Geotechnique 38(1):83–100

Kelly RB (2008) Back analysis of the Cumbalum trial embankment. Aust Geomech 43(1):47–54

Kelly RB, Wong PK (2009) An embankment constructed using vacuum consolidation. Aust Geomech 44(2):55–64

Kim R, Choi Y, Lee J, Lee W (2010) Evaluation of the PVD smear zone using micro penetrometer. In: GeoFlorida 2010: advances in analysis, modelling and design (GSP 199). American Society of Civil Engineers, New York, pp 998–1007, 20–24 Feb 2010

Kimoto S, Oka F (2005) An elasto-viscoplastic model for clay considering destructuralisation and consolidation analysis of unstable behaviour. Soils Found 45(2):29–42

Le TM, Fatahi B, Khabbaz H (2012) Viscous behaviour of soft clay and inducing factors. Geotech Geol Eng 30(5): 1069–1083

Leroueil S (1997) Closure to 'compressibility of clays: fundamental and practical aspects. J Geotech Geoenviron Eng 123(9):895

Mandel J (1953) Consolidation des sols (Etude Mathematique). Geotech 3(7):287–299

Marti J, Cundall P (1982) Mixed discretization procedure for accurate modelling of plastic collapse. Int J Numer Anal Meth Geomech 6(1):129–139

Mesri G, Lo DOK, Feng T-W (1994) Settlement of embankments on soft clays. In: vertical and horizontal deformations of foundations and embankments proceedings of settlement 94, GSP 40, ASCE, New York, pp 8–56

Muller R, Larssen S (2009) Veda trial embankment-comparison between measured and calculated deformations and pore pressure development. In: Leoni K (ed) Geotechnics of soft soils—focus on ground improvement. Taylor and Francis Group, London, pp 405–410

Nguyen L, Fatahi B, Khabbaz H (2014) A constitutive model for cemented clays capturing cementation degradation. Int J Plast 56:1–18

Onoue A, Ting NH, Germaine JT, Whitman RV (1991) Permeability of disturbed zone around vertical drains. In: Proceedings of the geotechnical engineering congress (GSP 27), American Society of Civil Engineers, New York, pp 879–890

Queensland Department of Transport SMS (1992) Performance of the trial embankment area 2A (Ch 28490-28640). Report R1802. Materials and Geotechnical Services Branch

Roscoe KH, Burland JB (1968) On the generalised stress–strain behaviour of 'wet clay', Engineering Plasticity. In: Heyman and Leckie (ed), pp 535–609

Rowe RK, Li AK (2002) Behaviour of reinforced embankments on soft rate sensitive soils. Geotechnique 52(1):859–869

Rowe RK, Taechakumthorn C (2008) Combined effect of PVDs and reinforcement on embankments over rate-sensitive soils. Geotext Geomembr 26(3):239–249

RTA (2000) Trial embnakment construction report. Roads and Traffic Authority of NSW, Pacific highway office, Grafton

Rujikiatkamjorn C, Indraratna B (2009) Design procedure for vertical drains considering a linear variation of lateral permeability within the smear zone. Can Geotech J 46(3): 270–280

Saowapakpiboon J, Bergado DT, Chai JC, Kovittayanon N, Zwart TP (2009) Vacuum-PVD combination with embankment loading consolidation in soft Bangkok Clay: a case study of the suvarnabhumi airport project. Paper presented at the 4th asian regional conference on geosynthetics, Shanghai, China

Saowapakpiboon J, Bergado DT, Voottipruex P, Lam LG, Nakakuma K (2011) PVD improvement combined with surcharge and vacuum preloading including simulations. Geotext Geomembr 29(1):74–82

Sathananthan I, Indraratna B, Rujikiatkamjorn C (2008) Evaluation of smear zone extent surrounding mandrel driven vertical drains using the cavity expansion theory. Int J Geomech 8(6):355–365

Schiffman RL, Chen AT-F, Jordan JC (1969) An analysis of consolidation theories. J Soil Mech Found Div 95(SM1):285–312

Sharma JS, Xiao D (2000) Characterization of a smear zone around vertical drains by large-scale laboratory tests. Can Geotech J 37(6):1265–1271

Stapelfeldt T, Vepsäläinen P, Yin ZY Numerical modelling of a test embankment on soft clay improved with vertical drains. In: KL (ed) Second international workshop on geotechnics of soft soils, Glasgow, Scotland, 3–5 Sept 2008. Taylor and Francis Group, London, pp 173–179

Tabatabaiefar S, Fatahi B, Samali B (2013a) Seismic behavior of building frames considering dynamic soil–structure interaction. Int J Geomech 13(4):409–420

Tabatabaiefar S, Fatahi B, Samali B (2013b) Lateral seismic response of building frames considering dynamic soil-structure interaction effects. Struct Eng Mech Int J 45(3):311–321

Tran-Nguyen HH, Edil TB (2011) The characteristics of PVD smear zone. In: Geo-Frontiers 2011: advances in geotechnical engineering, 13–16 March 2011. American Society of Civil Engineers, New York, pp 748–757. doi:10.1061/41165(397)77

Yan S-W, Chu J (2005) Soil improvement for a storage yard using the combined vacuum and fill preloading method. Can Geotech J 42(4):1094–1104

Yin J-H, Graham J (1989) Viscous-elastic-plastic modelling of one-dimensional time-dependent behaviour. Can Geotech J 26(2):199–209